

High efficiency and high transmission asymmetric polarization converter with chiral metasurface in visible and near-infrared region

Yuhang Gao(高雨航), Yu Tian(田宇), Qingguo Du(杜庆国), Yuanli Wang(王原丽), Qin Fu(付琴), Qiang Bian(卞强), Zhengying Li(李政颖), Shuai Feng(冯帅), and Fangfang Ren(任芳芳)

Citation: Chin. Phys. B, 2023, 32 (**7**): 074201. DOI: 10.1088/1674-1056/acb9eb
Journal homepage: http://cpb.iphy.ac.cn; http://iopscience.iop.org/cpb

What follows is a list of articles you may be interested in

Theoretical research on the transverse spin of structured optical fields inside a waveguide

Zhiyong Wang(王智勇), Xiangru Wang(汪相如), Anran Li(李岸然), Kaiqiang Zhang(张开强), Yukun Ji(纪玉坤), and Mingyu Zhong(钟明玉)

Chin. Phys. B, 2023, 32 (**6**): 064207. DOI: 10.1088/1674-1056/acbf28

Optically pumped wavelength-tunable lasing from a GaN beam cavity with an integrated Joule heater pivoted on Si

Feifei Qin(秦飞飞), Yang Sun(孙阳), Ying Yang(杨颖), Xin Li(李欣), Xu Wang(王旭), Junfeng Lu(卢俊峰), Yongjin Wang(王永进), and Gangyi Zhu(朱刚毅)

Chin. Phys. B, 2023, 32 (**5**): 054210. DOI: 10.1088/1674-1056/acc05e

Synthesis, magnetic and electromagnetic wave absorption properties of planar anisotrop Y_2Co_{17}@SiO_2 rare earth soft magnetic composites

Liang Qiao(乔亮), Cheng-Fa Tu(涂成发), Wei Wu(吴伟), Wen-Biao Wang(王文彪), Sheng-Yu Yang(杨晟宇), Sun Zhe(孙哲), Peng Wu(吴鹏), Jin-Bo Yang(杨金波), Chang-Sheng Wang(王常生), Tao Wang(王涛), and Fa-Shen Li(李发伸)

Chin. Phys. B, 2023, 32 (**5**): 054202. DOI: 10.1088/1674-1056/aca7f1

Size effect on light propagation modulation near band edges in one-dimensional periodic structures

Yang Tang(唐洋), Jiajun Wang(王佳俊), Xingqi Zhao(赵星棋), Tongyu Li(李同宇), and Lei Shi(石磊)

Chin. Phys. B, 2023, 32 (**5**): 054201. DOI: 10.1088/1674-1056/acac0d

Propagation of light near the band edge in one-dimensional multilayers

Yang Tang(唐洋), Lingjie Fan(范灵杰), Yanbin Zhang(张彦彬), Tongyu Li(李同宇), Tangyao Shen(沈唐尧), and Lei Shi(石磊)

Chin. Phys. B, 2023, 32 (**4**): 044209. DOI: 10.1088/1674-1056/ac892b

---

High efficiency and high transmission asymmetric polarization converter with chiral metasurface in visible and near-infrared region

Yuhang Gao(高雨航)[1], Yu Tian(田宇)[1], Qingguo Du(杜庆国)[1,†], Yuanli Wang(王原丽)[1,‡], Qin Fu(付琴)[1], Qiang Bian(卞强)[2], Zhengying Li(李政颖)[1,3], Shuai Feng(冯帅)[4], and Fangfang Ren(任芳芳)[5,§]

[1] *School of Information Engineering, Wuhan University of Technology, Wuhan* 430070, *China*
[2] *School of Electrical Engineering, Navy University of Engineering, Wuhan* 430033, *China*
[3] *National Engineering Research Center of Optical Fiber Sensing Technology and Networks, Wuhan* 430070, *China*
[4] *School of Science, Minzu University of China, Beijing* 100081, *China*
[5] *School of Electronic Science and Engineering, Nanjing University, Nanjing* 210023, *China*

(Received 25 November 2022; revised manuscript received 29 January 2023; accepted manuscript online 8 February 2023)

Polarization manipulation of light is of great importance because it could promote development of wireless communications, biosensing, and polarization imaging. In order to use natural light more efficiently, it is highly demanded to design and fabricate high performance asymmetric polarization converters which could covert the natural light to one particular linearly polarized light with high efficiency. Traditionally, polarizers could be achieved by controllers with crystals and polymers exhibiting birefringence. However, the polarizers are bulky in size and the theoretical conversion efficiency of the polarizers is limited to 0.5 with unpolarized light incidence. In this paper, we propose a polarization converter which could preserve high transmission for one linearly polarized light and convert the orthogonal linearly polarized light to its cross-polarized with high transmittance based on a multi-layer chiral metasurface. Theoretical results show that normally incident *y*-polarized light preserves high transmittance for the wavelength range from 685 nm to 800 nm while the orthogonal normally incident *x*-polarized light is efficiently converted to the *y*-polarized light with high transmittance from 725 nm to 748 nm. Accordingly, for unpolarized light incidence, transmittance larger than 0.5 has been successfully achieved in a broadband wavelength range from 712 nm to 773 nm with a maximum transmittance of 0.58 at 732 nm.

Keywords: asymmetric polarization converter, visible and near-infrared light, chiral metasurface, Fabry–Perot like resonance

PACS: 42.25.Bs, 42.81.Gs, 81.05.Xj **DOI:** 10.1088/1674-1056/acb9eb

1. Introduction

Polarization, one of the most important characteristics of electromagnetic waves, has been widely applied in many fields such as wireless communications,[1–4] biosensing,[5–7] and polarization imaging.[8–11] Especially, linearly polarized light is normally required for polarized light therapy,[12] head-up display system,[13] and LCD/OLED applications.[14] Hence, it is highly demanded to design and fabricate high performance polarization converters which could covert the natural light to one particular linearly polarized light with high efficiency to use the natural light more efficiently. Traditionally, polarization state of light could be manipulated by controllers with crystals and polymers exhibiting birefringence.[15] For example, polarizer could convert unpolarized light to linear polarized light by absorbing the light component with polarization perpendicular to the transmission axis, and allow the light component with polarization parallel to the transmission axis passing through. However, polarizers with birefringent crystals/polymers require long propagation distance to obtain phase accumulation which makes the polarizer too bulky for compact devices. Moreover, such polarizers usually encounter low efficiency and high loss.[16,17] The maximum efficiency of the polarizers in theory is only 0.5, which means that at least half of the incident optical energy will be wasted.

Over the past decade, metasurface, planar optical components consisting of patterned nanostructures at subwavelength scale, provides us a variety of opportunities to manipulate amplitude, phase and polarization of light with highly customized meta-atoms.[18–20] Chiral metasurface has been demonstrated to have giant chiroptical effect with optical activity much stronger than that of the natural chiral media.[21–25] Based on chiral metasurface, many different polarization converters have been proposed.[26,27] Asymmetric polarization converter based on metasurface, which has the capability to convert two orthogonal linearly polarized lights with different manner, has shown potential possibility to fabricate a compact and efficient polarizer to surpass the theoretical limit of the conventional polarizers.[28] Recently, several related works realizing asymmetric polarization conversion with chiral metasurface have been reported. Xu and co-workers realized asymmetric polarization conversion of two orthogonal linearly polarized waves around 0.53 THz.[26] Stephen and co-workers demonstrated an

†Corresponding author. E-mail: qingguo.du@whut.edu.cn
‡Corresponding author. E-mail: yuanliwang@whut.edu.cn
§Corresponding author. E-mail: ffren@nju.edu.cn

© 2023 Chinese Physical Society and IOP Publishing Ltd

asymmetric polarization conversion for two orthogonal linear polarized lights.[29] The proposed structure shows high conversion efficiency of one linearly polarized light to its orthogonal with high transmittance. However, the orthogonal linearly polarized incident light is mostly reflected rather than transmitted. Polarizers based on these structures still suffer from low total linear transmission efficiency of unpolarized incident light. Zhang and co-workers demonstrated a polarizer achieving a total transmission efficiency of 0.44 for linearly polarized transmittance with unpolarized light incidence around 1100 nm.[30] With the development of nanofabrication technology, the research of metasurface has been further developed to design and fabricate high-performance devices working in higher frequency range such as infrared and even visible.[31,32]

In this paper, we propose an asymmetric polarization converter based on multi-layer chiral metasurface which preserves high transmission for one linearly polarized light and convert the orthogonal linearly polarized light to its cross-polarized light with high transmittance. Theoretical results show that normally incident y-polarized light preserves high transmittance within the working bandwidth from 685 nm to 800 nm while the orthogonal normally incident x-polarized light is efficiently converted to the y-polarized light with high transmittance within the working bandwidth from 725 nm to 748 nm. For unpolarized incident light, transmittance larger than 0.5 has been successfully achieved for y-polarized light in a broadband wavelength range from 712 nm to 773 nm with a maximum total y-polarized transmittance of 0.58 at 732 nm. The mechanisms of asymmetric transmission for two orthogonal linear polarized light beams have been analyzed in detail. Finally, the surface current distributions are calculated to provide an intuitive image of the coupling between incident light and the metasurface at the resonant wavelength.

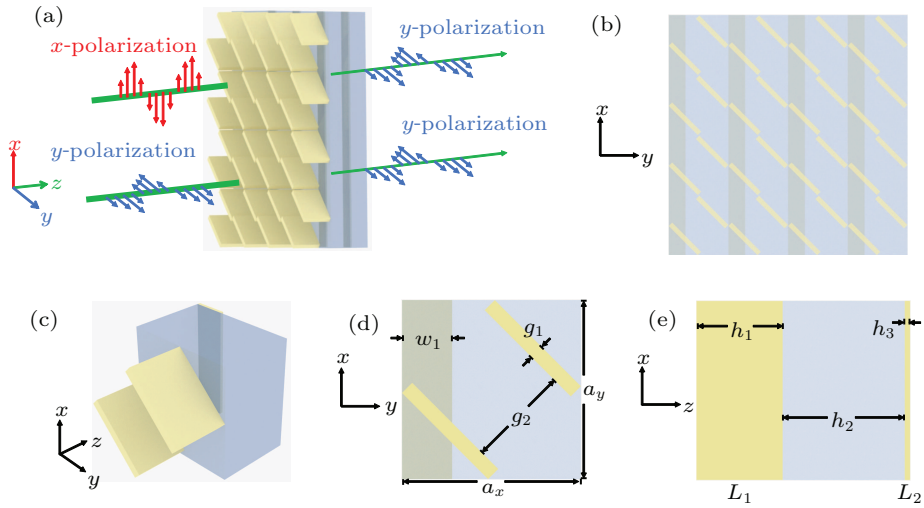


Fig. 1. Schematic diagram of the proposed asymmetric polarization converter. (a) Three-dimensional structure of 4×4 unit. (b) Top view of the structure in x–y plane of 4×4 unit. (c) Three-dimensional structure of one unit cell. (d) Top view of the structure in x–y plane of one unit cell. (e) Side view of the structure in x–z plane of one unit cell.

2. Device structure and methodology

The schematics of the proposed asymmetric polarization converter are shown in Fig. 1, which consists of parallel plates, rectangular gratings, and a dielectric layer inserted between them. Three-dimensional (3D) schematic diagram of 4×4 unit is illustrated in Fig. 1(a) with light propagation direction indicated. The x, y and z directions are indicated by red, blue, and green arrows, respectively. The colors of linearly polarized light are corresponding to the color of the respective axes. Top view of the structure in x–y plane of 4×4 unit is shown in Fig. 1(b). Figure 1(c) indicates a three-dimensional (3D) schematic diagram of one unit cell. Figure 1(d) indicates the top view of the structure in x–y plane. The width of the parallel plates and the gap between them are indicated as g_1 and g_2, respectively. The width of the rectangular grating is indicated as w_1. The period of the unit cell in x and y directions are indicated as a_x and a_y, respectively, which are both fixed at 500 nm. Figure 1(e) shows the side view of the structure, and the thicknesses of layers are indicated as h_1, h_2, and h_3, respectively. The top parallel plates and bottom rectangular grating are indicated as L_1 and L_2, respectively. Silica (SiO_2) is used as the material of the substrate with a relative permittivity of 2.1[33] and gold (Au) is employed as the material of top parallel plates and bottom rectangular grating with Drude model that is given in the following equation:[34]

$$\varepsilon(\omega) = 1 - \frac{\omega_p^2}{\omega(\omega + i\omega_\tau)}, \tag{1}$$

where $\omega_p = 1.37 \times 10^{16}$ Hz and $\omega_\tau = 4.08 \times 10^{13}$ Hz are plasma frequency and collision frequency, respectively. Modeling and simulation analyses are performed with the finite-difference time-domain (FDTD) method. Periodic boundary conditions and perfect matched layer are applied in x, y, and z directions, respectively.[35] To improve the accuracy of the

simulation, inhomogeneous mesh settings are applied in the simulation region. A finer mesh size is applied at the interfaces between the metal and the dielectric layer, which is set as 10 nm in x and y directions and 1 nm in the z direction. A mesh grid of 15 nm is applied to rest of the simulation region. Polarized light is vertically transmitted through the structure in the z direction from the parallel plates side.

3. Results and discussion

In order to analyze the optical characteristics of the designed metasurface, Jones matrix are used to describe the transmission properties with[36]

$$t_{xx} = |E_{xt}/E_{xi}|^2, \tag{2}$$
$$t_{yx} = |E_{yt}/E_{xi}|^2, \tag{3}$$
$$t_{xy} = |E_{xt}/E_{yi}|^2, \tag{4}$$
$$t_{yy} = |E_{yt}/E_{yi}|^2, \tag{5}$$

where t_{xx} or t_{yy} represents co-polarization transmittance of x- or y-polarized light, respectively, which evaluates the performance of polarization status preservation after passing through the metasurface structure, t_{yx} or t_{xy} represents cross-polarization transmittance of x- or y-polarized light, respectively, which evaluates the performance of polarization status conversion. E_{xi} is the amplitude of the incident x-polarized light and E_{xt} is the amplitude of the transmitted x-polarized light. E_{yi} is the amplitude of the incident y-polarized light and E_{yt} is the amplitude of the transmitted y-polarized light. Figure 2 shows the co- and cross-polarized transmittance spectra of x- and y-polarized light through the proposed metasurface structure. The cross-polarization transmittance t_{yx} is larger than 0.5 for the wavelength in the range of 725–748 nm with a maximum of 0.53 at the resonant wavelength of 736 nm, while the co-polarization transmittance t_{xx} is close to 0 at the same wavelength. The co-polarization transmittance t_{yy} is larger than 0.5 in the wavelength range from 685 nm to 800 nm with a maximum transmittance of 0.65 at the resonant wavelength of 720 nm, while the cross-polarization transmittance t_{xy} is close to 0 at the same wavelength. With respect to the unpolarized incident light, the total power transmission of light in y-polarization state $t_y = (t_{yx} + t_{yy})/2$ is larger than 0.5 in the wavelength range from 712 nm to 773 nm with a peak value of 0.58 at 732 nm.[30] Accordingly, the proposed metasurface can effectively convert the incident x-polarized light into its orthogonal polarized light, while the incident y-polarized light mostly maintains the original polarization state after passing through the structure. Asymmetrical manipulation of the polarization status of two orthogonal linearly polarized light beams has been successfully achieved, which means that the energy of the two linearly polarized light could be concentrate into one specific polarized light with reduced energy loss compared to the traditional polarizers.[37,38]

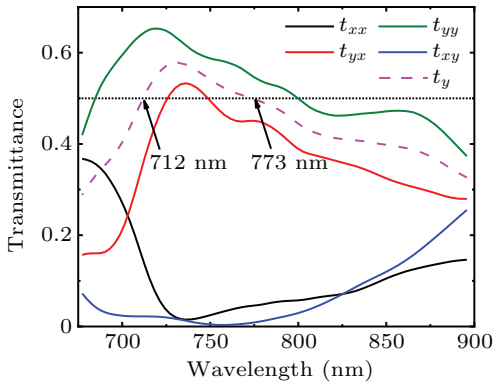


Fig. 2. Co- and cross-polarized transmittance and total transmittance in y-polarization state for an unpolarized light incidence of the proposed metasurface.

To further verify the asymmetric conversion performance of the metasurface structure, polarization azimuth angle θ and ellipticity angle η are further studied. Polarization azimuth angle θ that represents the rotation angle of the polarization plane of the transmitted light is normally used to evaluate the rotation ability of the metasurface to the polarization plane of incident light. Ellipticity angle η is normally used to evaluate the polarization status of the light, which is defined as the differential transmission between left-handed circularly polarized and right-handed circularly polarized light. Azimuth angle θ and ellipticity angle η are obtained as follows:[39]

$$\theta = [\arg(T_{++}) - \arg(T_{--})]/2, \tag{6}$$
$$\eta = \arctan[(|T_{++}| - |T_{--}|)/(|T_{++}| + |T_{--}|)], \tag{7}$$

where the circular transmission coefficients $T_{++/--}$ can be derived from the linear polarization transmission coefficients by $T_{++/--} = [T_{xx} + T_{yy} \pm \mathrm{i}(T_{xy} - T_{yx})]/2$. When $\theta = 90°$, the polarization plane of the transmitted light has been rotated for 90°. When $\eta = 0$, the light is pure linearly polarized. As shown in Fig. 3, polarization azimuth angle θ is around 90° and ellipticity angle η is near 5° in the range of 725–748 nm. Accordingly, the transmitted light of incident x-polarized light is linearly polarized light and the polarization plane has been rotated for 90°.

In order to analyze the effect of chirality, we further study the transmission and absorption differences between left and right circularly polarizations. Figure 4(a) shows the transmittance spectra of left and right circularly polarized light. In Fig. 4(a), $t_{++/--}$ represent the circularly polarized transmittance, where $++$ and $--$ represent right and left circularly polarizations, respectively. The difference of the circularly polarized transmittance can be obtained by the equation $\Delta t = t_{++} - t_{--}$. The right circularly polarized transmittance (t_{++}) is larger than the left circularly polarized transmittance (t_{--}) in the wavelength range from 675 nm to 900 nm. Δt reaches

a peak value of 0.51 at 733 nm, while t_{yx} reaches a peak value of 0.53 at 736 nm according to Fig. 2. From Fig. 4(a), large transmission difference between the left and right circularly polarized components of an incoming linearly polarized light has been obtained to be of the proposed chiral structure. In Fig. 4(b), $A_{++/--}$ represent the absorption of right and left circularly polarizations, respectively. The difference of the circular absorption which represents circular dichroism (CD) can be obtained by the equation $\Delta A = A_{--} - A_{++}$. As shown in Fig. 4(b), the absorption of left circularly polarized component is larger than the right circularly polarized component in the wavelength range from 675 nm to 900 nm. The difference of the circular absorption reaches a peak value of 0.37 at 716 nm. Transmission and absorption differences between the left and right circularly polarized components of an incoming linearly polarized light finally lead to high cross-polarized transmittance of t_{yx}.

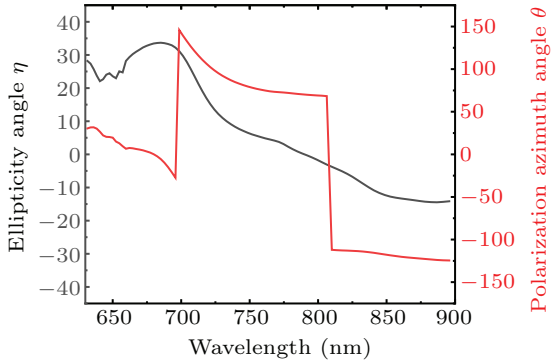


Fig. 3. Polarization azimuth angle θ and ellipticity angle η for x-polarized incident light.

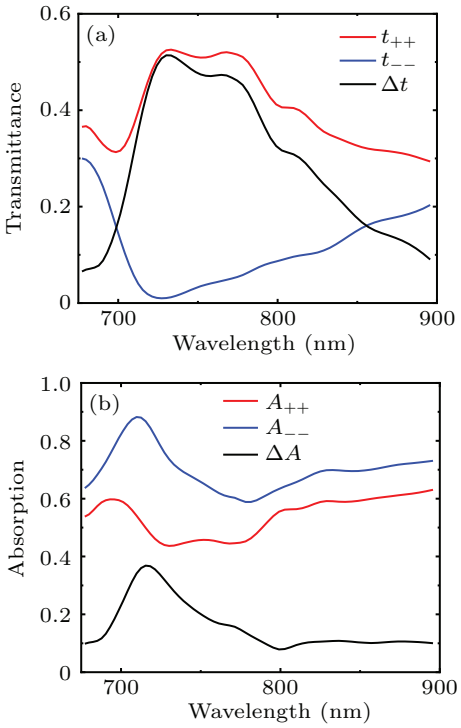


Fig. 4. Circularly polarized spectra. (a) Transmittance of left and right circularly polarized light. (b) Absorption of left and right circularly polarized light.

To identify the function of each individual layer and to clarify the intrinsic mechanisms, the transmittances of co- and cross-polarization of both x- and y-polarized incident light beams for L_1 only and for L_1L_2 (combining L_1 with L_2) are simulated as shown in Fig. 5. For the case of L_1 only, the co- and cross-polarization transmittances are almost identical to each other for x- and y-polarized incident light due to the lack of anisotropy of the single layer L_1. Both x- and y-polarized light beams could be converted to cross-polarized light. Clearly, there is no asymmetric polarization conversion with L_1 only. Consequently, L_1 simply works as a polarization converter. The co-polarization transmittance (t_{xx}, t_{yy}) and cross-polarization transmittance (t_{yx}, t_{xy}) are smaller than 0.5 in the whole wavelength range studied here. For the case of L_1L_2, as shown in Figs. 5(b) and 5(d), the cross-polarization transmittance t_{yx} and co-polarization transmittance t_{yy} are significantly improved, which lead to an asymmetric polarization manipulation in the wavelength range from 725 nm to 748 nm. We believe that the asymmetric polarization conversion is due to the symmetry breaking of the metasurface in the direction of propagation with the combination of L_1 and L_2.

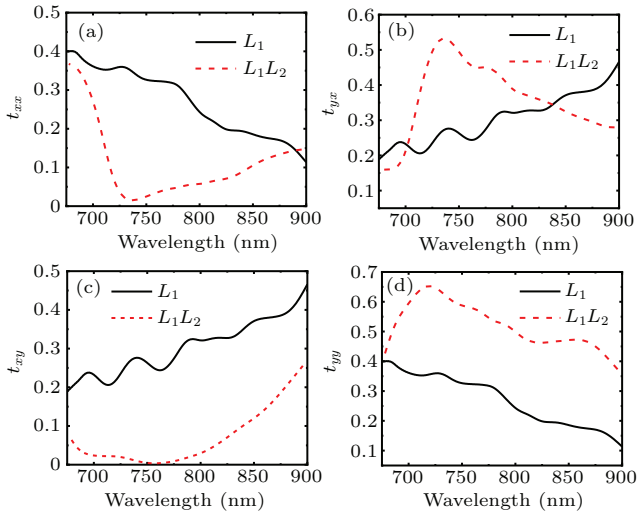


Fig. 5. Transmission spectra of L_1 and L_1L_2. [(a), (d)] Co-polarized transmittance t_{xx} and t_{yy}. [(b), (c)] Cross-polarized transmittance t_{yx}, t_{xy}.

Obviously, L_2 also play an important role for asymmetric polarization conversion. In order to fully understand the role of L_2, as shown in Fig. 6, we simulate and calculate the co- and cross-polarization transmittance and reflectance of both x- and y-polarized incident light beams. Clearly, the cross-polarized transmittance and cross-polarized reflectance are both nearly zero, denoting that the polarization status of the incident light cannot be rotated with L_2 only. As shown in Figs. 6(a) and 6(c), the co-polarized transmittance of x-polarized incident light is less than 0.1 and the co-polarized reflectance of x-polarized incident light is around 0.5 in the wavelength range of 725–748 nm, which means that L_2 works as a reflector for x-polarized incident light. On the other hand, as shown

in Figs. 6(b) and 6(d), the co-polarized transmittance of *y*-polarized incident light is above 0.85 while the co-polarized reflectance of *y*-polarized incident light is less than 0.1 in the same wavelength range, which indicates that most of the *y*-polarized incident light could transmit through L_2. L_2 with its long axis along the *y*-axis plays a role of polarization filter which allows the *y*-polarized light to pass through and reflects the *x*-polarized light.

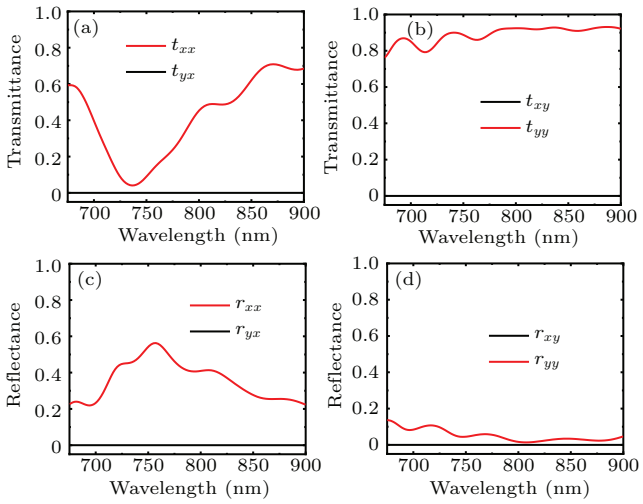


Fig. 6. Transmission and reflection spectra of L_2. (a) Co- and cross-transmittance of *x*-polarized incident light. (b) Co- and cross-transmittance of *y*-polarized incident light. (c) Co- and cross-reflectance of *x*-polarized incident light. (d) Co- and cross-reflectance of *y*-polarized incident light.

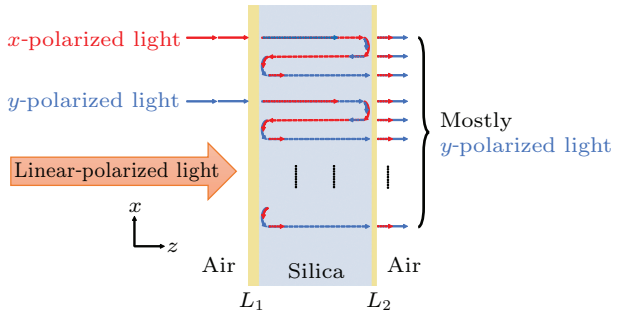


Fig. 7. Model of the Fabry–Pérot-like resonance in the proposed structure.

By combing the polarization conversion layer L_1 with the polarization filter layer L_2, a Fabry–Pérot-like resonance is formed in the metasurface structure.[40] As shown in Fig. 7, for the *x*-polarized light, after passing through L_1, the *x*-polarized light is partially converted to *y*-polarized light. Most of the converted *y*-polarized light is transmitted through L_2. The unconverted *x*-polarized light is reflected back to L_1 and continuously converts to *y*-polarized light. Finally, owing to the Fabry–Pérot-like resonator, the *x*-polarized light is mostly converted to *y*-polarized light. Similarly, for the *y*-polarized light, after passing through L_1, the *y*-polarized light is partially converted to *x*-polarized light. Most of the unconverted *y*-polarized light transmits through L_2, and the converted *x*-polarized light is mostly reflected back from L_2, which will be converted to *y*-polarized light by L_1. Finally, *y*-polarized light shows high co-polarized transmittance through L_1L_2. Accordingly, after passing through the proposed structure, *x*- and *y*-polarized light beams are both transmitted as *y*-polarized light.

In order to further justify the Fabry–Pérot-like resonance of the proposed structure, the influence of the dielectric substrate thickness h_2, which can be considered as the resonance distance of Fabry–Pérot model, is shown in Fig. 8. Clearly, it can be observed that the resonance wavelength of the cross-polarized transmittance for *x*-polarized incident light redshifts with the increasing h_2, conforming to the approximately linear relationship of the resonance distance of Fabry–Pérot model h_2 and the resonance wavelength λ. This observable periodic performance further justifies that the proposed structure has a Fabry–Pérot-like effect.[41] It is worth noting that the strong circular dichroism in both transmission and absorption shown in Fig. 4 is benefited from the Fabry–Pérot-like resonance, even though the resonant strength is limited.

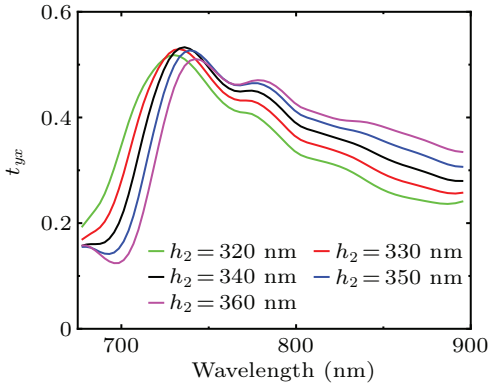


Fig. 8. Influence of the dielectric substrate thickness h_2.

In order to figure out the relationship between transmission performance and the structure period, we depict the influence of the structure period through three transmission spectra, as shown in Fig. 9. Cross-polarized transmittance for *x*-polarized incident light, co-polarized transmittance for *y*-polarized incident light, and total power transmittance of light in *y*-polarization state are plotted in Figs. 9(a)–9(c) for the structure periods of 400 nm, 500 nm, and 600 nm, respectively. As shown in Fig. 9(a), with the increasing period, the resonance wavelength of t_{yx} redshifts, while the resonance bandwidth and the peak value of t_{yx} are decreased. As shown in Fig. 9(b), the peak value of t_{yy} increases and the resonance wavelength of t_{yy} redshifts with the structure period increasing. As shown in Fig. 9(c), total power transmittance of light in *y*-polarization state is larger than 0.5 in the wavelength ranges of 689–723 nm, 712–773 nm, and 773–804 nm, corresponding to the structure periods of 400 nm, 500 nm, and 600 nm respectively. Total transmission of t_y gets a maximum transmittance of 0.53 at 707 nm, 0.58 at 732 nm, and 0.54 at 786 nm.

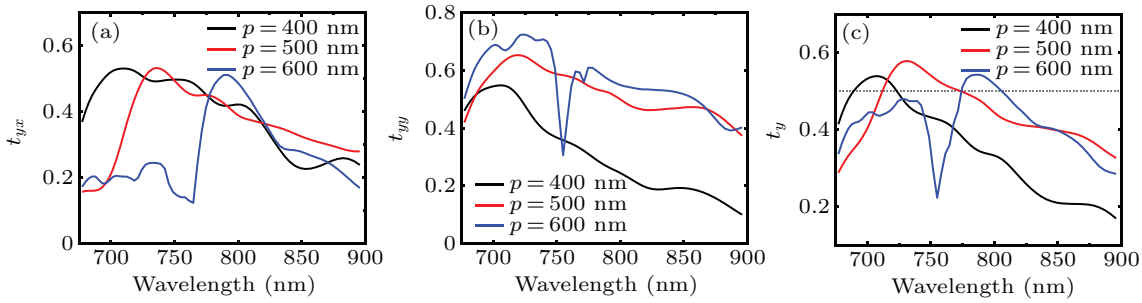


Fig. 9. Transmission spectra of different structure periods. (a) Cross-polarized transmittance for x-polarized incident light. (b) Co-polarized transmittance for y-polarized incident light. (c) Total power transmittance of light in y-polarization state.

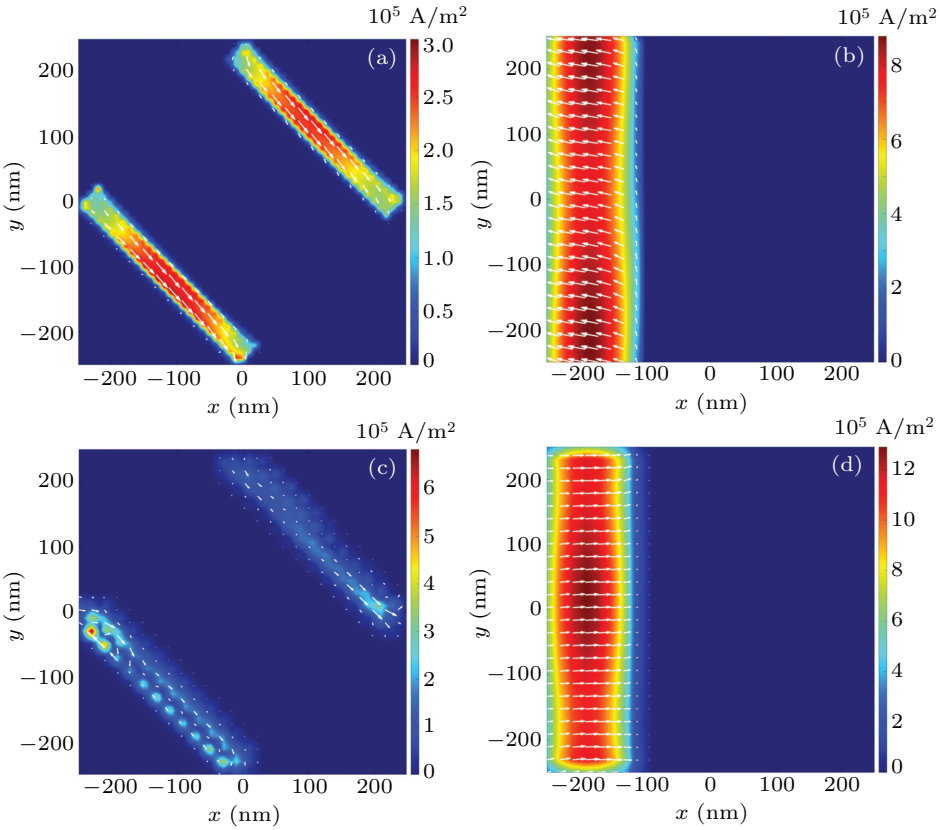


Fig. 10. The surface current distribution at L_1 and L_2 for [(a), (b)] x-polarized incident light, or [(c), (d)] y-polarized incident light at the wavelength of 736 nm.

To analyze the mechanism of the asymmetric polarization conversion in detail, surface current distributions on both L_1 and L_2 at the resonance wavelength of 736 nm are plotted in Figs. 10(a)–10(d). For x-polarized incident light, the instantaneous direction of the current flow of L_1 resonator is opposite to that of L_2, which indicates that an equivalent magnetic resonator is formed.[42] Strong coupling from anti-paralleled currents between L_1 and L_2 promotes the polarization rotation of the incident light.[43] For y-polarized incident light, instantaneous direction of the current flow of L_1 is almost the same as that of x-polarized incident light with much weaker intensity and the current flow in L_2 is nearly along the same direction as that in L_1. Accordingly, for y-polarized incident light, the equivalent magnetic resonator cannot be excited, which indicates that the y-polarized light could pass through the proposed metasurface structure with high transmittance within the working band.

4. Conclusion

In summary, we have proposed a polarization converter with efficient asymmetric polarization conversion for linearly polarized visible and near-infrared light based on a three-layered chiral metasurface. The proposed structure can efficiently convert the x-polarized incident light to its orthogonal y-polarized light and transmit most of the y-polarized incident light within the wavelength range from 725 nm to 748 nm. Meanwhile, y-polarized light preserves high transmittance within the working bandwidth from 685 nm to 800 nm after passing through the proposed metasurface structure. Accordingly, for unpolarized incident light, transmittance larger

than 0.5 has been successfully achieved in a broadband wavelength range from 712 nm to 773 nm with a maximum total y-polarized transmittance of 0.58 at 732 nm. Both the ellipticity angle and the polarization azimuth angle verify that the incident x-polarized light could be successfully converted to cross-polarized light. Transmission and absorption difference of the left and right circularly polarized components of an incoming linearly polarized light indicates the chiral performance, which further verifies the high polarization conversion efficiency. It is also demonstrated that the top parallel plates layer acts as the polarization conversion layer and the bottom rectangular grating layer acts as a polarization filter. The combination of top parallel plates layer and the bottom rectangular grating layer forms an Fabry–Pérot-like resonator, which further boosts the asymmetric polarized conversion efficiency. The redshifts of the resonance wavelength λ with the increasing resonance distance h_2 further verify the Fabry–Pérot-like resonance. Surface current distribution analysis reveals that anti-paralleled currents between top parallel plates layer and the bottom rectangular grating layer promote the polarization rotation, and paralleled currents result in high transmittance of the incident light. We believe that the designed metasurface provides a new route for designing compact and efficient optical asymmetric polarization converter for visible and near-infrared light with high transmittance, which could break the 0.5 limit of the conventional polarizers.

Acknowledgements

Project supported by the National Natural Science Foundation of China (Grant Nos. 62075173 and 12274478), and the National Key Research and Development Program of China (Grant Nos. 2021YFB2800302 and 2021YFB2800604).

References

[1] Fan J, Zhang L, Wu Z, Liang J, Ning T, Zhang M, Su H and Liang H 2022 *Opt. Laser Technol.* **151** 108064
[2] Jiang X, Fan W, Qin C and Chen X 2021 *Nanomaterials* **11** 2895
[3] Wang G, Shao L Y, Xiao D, Bandyopadhyay S, Jiang J, Liu S, Li W, Wang C and Yan Z 2021 *J. Lightwave Technol.* **39** 83
[4] Yu J Y, Zheng Q R, Zhang B, He J, Hu X M and Liu J 2022 *Chin. Phys. B* **31** 090704
[5] Zhang Z Y, Fan F and Li T F 2020 *Chin. Phys. B* **29** 078707
[6] Zhang M, Hao D, Wang S, Li R, Wang S, Ma Y, Moro R and Ma L 2022 *Opt. Express* **30** 14651
[7] Hu J, Lu J, Liang Z, Liu L, Wang W, Zhou P and Ye M 2022 *Biosensors* **12** 529
[8] Tian X, Liu R, Wang Z and Ma J 2022 *Inform. Fusion* **77** 19
[9] Wang S, Deng Z L, Wang Y, Zhou Q, Wang X, Cao Y, Guan B, Xiao S and Li, X 2021 *Light Sci. Appl.* **10** 24
[10] Ding X, Wang Y and Fu X 2022 *Opt. Laser Eng.* **152** 106971
[11] Liu X, Chang J, Feng S, Mu Y, Wang X and Xu Z P 2019 *Chin. Phys. B* **28** 084201
[12] Mohamed M H, Selem M N, Mohamed M S and Abd EL-Ghaffaar 2019 *Drug Invention Today* **11** 2945
[13] Zou J, Hsiang E L, Zhan T, Yin K, He Z and Wu S T 2020 *Opt. Express* **28** 24298
[14] Kim M, Lee D, Oh Y, Lee J. Y, Kim B, Park J, Park D and Hong W 2022 *IEEE Trans. Antenn. Propag.* **70** 5929
[15] Nose T, Sato S, Mizuno K, Bae J and Nozokido T 1997 *Appl. Opt.* **36** 6383
[16] Huang Y, Zhou Y and Wu S T 2007 *Opt. Express* **15** 6414
[17] Liu Y and Zhang X 2011 *Chem. Soc. Rev.* **40** 2494
[18] Fedotov V A, Mladyonov P L, Prosvirnin S L, Rogacheva A V, Chen Y and Zheludev N I 2006 *Phys. Rev. Lett.* **97** 167401
[19] Hu Y, Wang X, Luo X, Ou X, Li L, Chen Y, Yang P, Wang S and Duan H 2020 *Nanophotonics* **9** 3755
[20] Liu M, Zhu W, Huo P, Feng L, Song M, Zhang C, Chen L, Lezec H, Lu Y, Agrawal A and Xu T 2021 *Light Sci. Appl.* **10** 1
[21] Li Z, Zhao R, Koschny T, Kafesaki M, Alici K B, Colak E, Caglayan H, Ozbay E and Soukoulis C M 2010 *Appl. Phys. Lett.* **97** 081901
[22] Decker M, Klein M W, Wegener M and Linden S 2007 *Opt. Lett.* **32** 856
[23] Engelbrecht S, Wunderlich M, Shuvaev A M and Pimenov A 2010 *Appl. Phys. Lett.* **97** 081116
[24] Singh R, Plum E, Zhang W and Zheludev N I 2010 *Opt. Express* **18** 13425
[25] Yi C, Chen Z, Gao Y and Du Q 2022 *Opt. Express* **30** 10032
[26] Xu W Z, Shi Y T, Ye J, Ren F F, Shadrivov I V, Lu H, Liang L, Hu X, Jin B, Zhang R, Zheng Y, Tan H and Jagadish C 2017 *Adv. Opt. Mater.* **5** 1700108
[27] Han B, Li S, Li Z, Huang G, Tian J and Cao X 2021 *Opt. Express* **29** 19643
[28] Ding F, Pors A and Bozhevolnyi S I 2017 *Rep. Prog. Phys.* **81** 026401
[29] Stephen L, Yogesh N and Subramanian V 2018 *J. Appl. Phys.* **123** 033103
[30] Zhang Y, Yang L, Li X K, Wang Y L and Huang C P 2020 *J. Opt.* **22** 035101
[31] Li P, Chen S, Dai H, Yang Z, Chen Z, Wang Y, Chen Y, Peng W, Shan W and Duan H 2021 *Nanoscale* **13** 1529
[32] Jahani S and Jacob Z 2016 *Nat. Nanotechnol.* **11** 23
[33] Chen H, An D, Li Z and Zhao X 2017 *Opt. Express* **25** 26417
[34] Yelon A, Piyakis K N and Sacher E 2004 *Surf. Sci.* **569** 47
[35] Lin Z, Xu Z, Liu P, Liang Z and Lin Y 2020 *Opt. Laser Technol.* **121** 105826
[36] Menzel C, Rockstuhl C and Lederer F 2010 *Phys. Rev. A* **82** 053811
[37] Huang C P, Wang Y L and Zhang Y 2019 *J. Opt.* **21** 105001
[38] Mun S E, Hong J, Yun J G and Lee B 2019 *Sci. Rep.* **9** 2543
[39] Ren M X, Wu W, Cai W, Pi B, Zhang X Z and Xu J J 2017 *Light Sci. Appl.* **6** e16254
[40] Wang Y H, Jin R C, Li J, Li J Q and Dong Z G 2018 *Opt. Express* **26** 3508
[41] Trentini G V 1956 *IRE Trans. Anten. Propag.* **4** 666
[42] Liu W, Wu W, Huang L, Ling Y, Ba C, Li S, Chun Z and Li H 2019 *Opt. Express* **27** 33399
[43] Hentschel M, Weiss T, Bagheri S and Giessen H 2013 *Nano Lett.* **13** 4428